Acta Cryst. (1998). B**54**, 741–749

Equation of State of α-Al_2O_3 (Corundum) from Quasi-Harmonic Atomistic Simulations

Michele Catti[a]* and Alessandro Pavese[b]

[a]*Dipartimento di Scienza dei Materiali, Università di Milano, Via Emanueli 15, 20126 Milano, Italy, and* [b]*Dipartimento di Scienze della Terra (Sezione di Mineralogia), Università di Milano, Via Botticelli 23, 20133 Milano, Italy. E-mail: catti@mater.unimi.it*

(*Received 6 January 1998; accepted 5 March 1998*)

Abstract

A two-body interatomic potential function, including fractional atomic charges and a shell model for oxygen, and supplemented by an O—Al—O bond-angle energy term, was fitted to the structural, elastic and vibrational properties of α-Al_2O_3, corundum, at ambient conditions. Full quasi-harmonic calculations were then carried out on a p,T grid of 54 points in the domain 0–40 GPa and 300–1700 K. The crystal structure was equilibrated at each point, taking into account the anisotropy of vibrational pressure and the thermal dependence of elastic constants, so as to obtain unit-cell edges, atomic coordinates, bulk modulus, thermal expansion coefficient and other thermodynamic properties. Polynomial approximations were developed to represent the p,T dependence of these quantities. Comparison with experimental results for the separate p (T = 300 K) and T (p = 0) behaviours shows very good agreement, with average deviations of 0.1% for the unit-cell volume and 6% for the thermal expansion coefficient. The coupled p,T dependence of the properties of corundum is predicted to be very small for the bulk modulus ($\partial^2 K_T/\partial p \partial T = 8.4 \times 10^{-5}$ K^{-1}), but not at all negligible for the volume [$(1/V)\partial^2 V/\partial p \partial T$ in the range -1.2 to -7.5×10^{-7} GPa^{-1} K^{-1} over the p,T domain explored].

1. Introduction

A new interest has arisen recently in the p,T equation of state of crystalline materials, owing to the modern performances of diffraction techniques at high temperature/high pressure afforded by the use of neutron and synchrotron X-ray sources (Hull *et al.*, 1997; Zhang *et al.*, 1997). However, in most cases experiments are still performed either at variable temperature or at variable pressure; changing both quantities together may limit the accuracy of results and/or the explored p,T range. Thus, it can be very useful to have theoretical results available for two purposes: first, to check theory against accurately measured data *versus* either T or p; second, to predict the coupled p,T behaviour, so as to also have guidelines for planning experiments *versus* simultaneously varied T and p.

The theoretical approach which seems to best suit these requirements is the quasi-harmonic model of crystalline solids (Born & Huang, 1954), provided that the temperature range considered is far enough from the melting point. In this approach the full spectrum of vibrational frequencies of the solid is calculated at several volumes or deformation states of the crystal lattice, deriving the corresponding thermodynamic properties on the basis of standard statistical mechanics formalism. Computations are carried out in the frame of an atomistic model, where the atom–atom potential energy is expressed by a simple formula containing empirically fitted parameters. Minimization of the free energy leads to knowledge of the full p,T dependence of unit-cell constants and of atomic coordinates. We applied this approach to study the thermal expansion of calcite, $CaCO_3$, at ambient pressure (Catti *et al.*, 1993; Pavese *et al.*, 1996).

Corundum (α-Al_2O_3) was selected for an investigation of the full p,T equation of state for a number of reasons. Indeed, its applications as a refractory material and as a support for catalysts, and its relevant role as a mineral in earth sciences are well known. Further, α-alumina is an important standard substance often used for calibration purposes in diffraction experiments. In all these cases a knowledge of the full dependence of the crystal structure on p,T would be highly desirable. Several experimental data for thermal expansion at room pressure are available in the literature: some of them originate from interferometric measurements (Wachtman *et al.*, 1962; Yates *et al.*, 1972) and others from X-ray diffraction (Touloukian *et al.*, 1977; Brown *et al.*, 1993). However, only a single structural refinement at high temperature (2170 K) is present (Ishizawa *et al.*, 1980), while of course there are many at room temperature (*cf. e.g.* Kirfel & Eichhorn, 1990; Lewis *et al.*, 1982). A number of papers report unit-cell compression results at room temperature by X-ray diffraction: diamond-anvil cell (DAC) data to 49.3 GPa (Richet *et al.*, 1988); cubic anvil data to 12 GPa (Sato & Akimoto, 1979); DAC data with synchrotron radiation in the range 68–175 GPa (Jephcoat *et al.*, 1988). Single-crystal DAC structural results to 9 GPa are reported by d'Amour *et al.* (1978). Eventually, the elastic constants

ISSN 0108-7681

and bulk modulus were measured in the T range from 300 to 1800 K by the rectangular parallelepiped resonance method (Goto & Anderson, 1989). No experimental results exist, to our knowledge, for the simultaneous p,T dependence of lattice and elastic data.

Previous simulations of corundum properties based on model interatomic potentials include the work of Catlow *et al.* (1982) and Schober *et al.* (1993). The first paper aimed mainly at the calculation of point defect energetics; the potential developed therein will be taken into account as a starting point for this work. In the second paper the principal objective was fitting and interpreting the lattice-dynamical results of inelastic neutron diffraction experiments. In the present investigation we first want to develop an improved shell-model potential for α-Al_2O_3 by including the effect of vibrational frequencies and of possible O—Al—O bond-bending terms. Then the modified version of the *PARAPOCS* code, which fully accounts for the anisotropy of the thermal pressure and thermal dependence of elastic properties (Pavese *et al.*, 1996; Parker & Price, 1989), will be applied for the first time to the computation of the high p,T equation of state of a crystal.

2. Computational method

At thermodynamic equilibrium the anisotropic equation of state for a crystalline solid is

$$\tau_i = (1/V)(\partial F/\partial \varepsilon_i)_{T,\varepsilon_j} = \tau_i(\varepsilon_1, \ldots \varepsilon_6, T), (i = 1, \ldots 6), \tag{1}$$

where τ_i and ε_i are the stress and strain components, respectively, in the Voigt notation and F is the Helmholtz free energy. Strain components are related to changes of the lattice constants. By assuming a microscopic atomistic model based on interatomic potential energy functions, and expressing the vibrational part of the free energy in the frame of the quasi-harmonic approximation, it is possible to compute the vibrational frequencies $\omega_{n\mathbf{K}}$ for every phonon branch n and wavevector $\mathbf{K}$ and thus to obtain F as a function of T, of the atomic coordinates and of the lattice strain components ε_i. Straightforward differentiation yields the lattice stresses, according to (1). The particular case of isotropic pressure p corresponds to $\tau_i = -p$ (i = 1,2,3) and $\tau_i = 0$ (i = 4,5,6).

The problem is inverting (1) to obtain the strain components as functions of the stress, because in most cases the piece of information required is the evolution of the lattice geometry with temperature and pressure. This is usually performed by solving (1), considered as equations in the unknowns ε_i, by an iterative linear approximation (Newton method),

$$\varepsilon_i = \sum_{j=1}^{6} s_{ij}\tau_j, \tag{2}$$

where s_{ij} are components of the 6×6 matrix of elastic compliances $\mathbf{s} = \mathbf{C}^{-1}$ and the elastic constants C_{ij} are second derivatives of the free energy with respect to strain components, divided by the volume.

The free energy can be split into a static and a vibrational part, which are T independent and T dependent, respectively,

$$F = E_{\rm st} + F_{\rm vib}(T); \tag{3}$$

correspondingly

$$\begin{aligned}\tau_i &= (1/V)(\partial E_{\rm st}/\partial \varepsilon_i) + (1/V)(\partial F_{\rm vib}/\partial \varepsilon_i)_{T,\varepsilon_j} \\ &= \tau_i({\rm st}) + \tau_i({\rm vib}),\end{aligned} \tag{4}$$

and a similar splitting is obtained for the elastic constants. Thus, for an initial unit-cell geometry the first (τ_i) and second (C_{ij}) derivatives of F are computed, and the corresponding strain (2) gives a new better approximation for the unit-cell constants. The process is repeated until the computed stresses are equal to the external ones. At each cycle the condition of minimum F with respect to atomic coordinates has to be fulfilled.

3. Interatomic potential

The classical Born-type form of the two-body interatomic (electrostatic + repulsive) potential,

$$E_{ij} = e^2 z_i z_j / r_{ij} + A_{ij} \exp(-r_{ij}/\rho_{ij}),$$

was assumed, supplemented by a dispersion attractive term $-c_{ij}/r_{ij}^6$ for O—O interactions only. A shell model was used for O atoms, taking into account the electronic polarization. Both core and shell positions are involved in computing the electrostatic energy [except for the intra-atomic core-shell interaction, which is accounted for by the elastic energy $(1/2)k_{\rm cs}r_{\rm cs}^2$]; only shell positions are used to calculate repulsion and dispersion energies. The repulsive parameters A_{ij} and ρ_{ij} for each pair of atomic species, the $c_{\rm O-O}$ coefficient, the two electric charges z_s and z_c for the O shell and core (the Al charge is constrained by electroneutrality), and the $k_{\rm cs}$ core-shell spring constant have to be determined empirically and they are denoted collectively as p_i (i = 1,...10). Such parameters were fitted to the following observables: a and c unit-cell edges, x(O) and z(Al) atomic fractional coordinates (Kirfel & Eichhorn, 1990), six elastic constants (Goto & Anderson, 1989), and 18 zone-centre ($\mathbf{K}$ = 0) vibrational frequencies from Raman and IR spectroscopy (nine of non-degenerate A and nine of doubly degenerate E type, accounting for 27 internal degrees of freedom; Kappus, 1975). Indeed, the stress components τ_1 and τ_3 (related to energy derivatives with respect to a and c) were considered, rather than a and c themselves; their 'observed' values are of course vanishing for the experimental crystal structure. All the above observables are indicated collectively as

Table 1. *Parameters of the potential optimized for α-Al_2O_3*

Pre-exponential factors A_{ij} and hardness parameters ρ_{ij} of repulsive energy, dispersive coefficient c_{ij}, atomic charges (shell and core values for O), core-shell force constant k_{cs} and three-body angular force constant k_{O-Al-O}.

	A_{ij} (eV)	ρ_{ij} (Å)	c_{ij} (eV Å^6)
O_s-O_s	80356.0	0.2072	125.5
Al—O_s	1843.2	0.2392	0
Al—Al	2721.9	0.0872	0

$z(O_s)$ (e)	−2.677
$z(O_c)$ (e)	1.529
z(Al) (e)	1.722
k_{cs} (eV Å^{-2})	155.2
k_{O-Al-O} (eV rad^{-2})	7.456

Table 2. *Observables [residual lattice stresses (GPa), atomic fractional coordinates and elastic constants (GPa)] used in the fitting of the interatomic potential, excluding the vibrational frequencies: final computed values compared with experimental values (Kirfel & Eichhorn, 1990; Goto & Anderson, 1989)*

	Calculated	Experimental
τ_1	−0.04	0
τ_3	0.16	0
x(O)	0.30857	0.30627
z(Al)	0.35836	0.35220
C_{11}	467.6	497.3
C_{33}	527.5	500.9
C_{44}	167.7	146.8
C_{12}	169.7	162.8
C_{13}	113.7	116.0
C_{14}	−14.9	−21.9

Q_k (k = 1,...28). The ten potential parameters p_i are optimized by minimization of the function $f(p_i) = \sum_k w_k[Q_{k,\mathrm{calc}}(p_i) - Q_{k,\mathrm{obs}}]^2$, where the w_k weights play not only a dimensional role, but also control the desired relative importance of different observables in the fitting process. All calculations were carried out by the modified version of the computer program *PARAPOCS* (Pavese *et al.*, 1996), which is able to produce all $Q_{k,\mathrm{calc}}$ quantities for a given set of p_i parameters, appropriately linked to the optimization routine *MINUIT* (James & Roos, 1975). Initially, the minimum of $f(p_i)$ was searched for by the simplexus method and it was later refined by the modified Newton approximation.

As starting values, the potential parameters developed by Catlow *et al.* (1982) with formal net atomic charges (+3 *e* on Al) were used. The first step of the optimization was purely static: *i.e.* the τ_1 and τ_3 stresses were computed as derivatives of the static lattice energy with respect to strain components. In the second step thermal effects on the unit cell at T = 300 K were introduced by computing the τ_1 and τ_3 stresses as derivatives of the Helmholtz free energy F. This meant including the numerical differentiation of all lattice-dynamical frequencies with respect to strain components, according to the quasi-harmonic model; 64 points in the first Brillouin zone were used to generate a total of 1920 frequencies. At convergence of the optimization process, a reasonable agreement was attained for all the observables involved. However, the residual stresses on the unit cell (τ_1 = −0.29, τ_3 = 0.55 GPa) were considered to be still large and thus we attempted to improve the interatomic potential by including three-body terms of the type O—Al—O and Al—O—Al, with a quadratic dependence on the deviation of the bond-bending angle from its ideal octahedral value. Repeating the whole optimization procedure showed that a real improvement was given by the O—Al—O term only, while the Al—O—Al potential was not influential and was thus omitted. The final optimized parameters are reported in Table 1 and the corresponding calculated values of the observables (excluding spectroscopic data) are compared with the experimental values in Table 2. The 18 vibrational frequencies, not reported for brevity, range from 10 to 26 THz and show an average and maximum relative deviation from measured values of 5.0 and 11.9%, respectively. Much smaller residual stresses are now observed and also the C_{12} and C_{13} elastic constants and several zone-centre vibrational frequencies are significantly improved by the effect of the O—Al—O three-body potential term. In comparison with the results obtained by Catlow *et al.* (1982), who fitted their potential statically only without considering the vibrational frequencies, a great improvement is observed for most of the relevant observables, in particular C_{12}, C_{13} and C_{14}. The atomic net charges deviate significantly from their formal values, indicating that their relaxation is important to obtain a good potential. As a further test of the quality of the potential, off-zone-centre phonon frequencies were computed along the [001] direction ($\Gamma - Z$) in reciprocal space, at $K_3/2\pi c^*$ = 0.1, 0.2, 0.3, 0.4, and compared with experimental results from inelastic neutron scattering (Schober *et al.*, 1993). The average relative deviations, calculated over 20 frequency values (of which ten are doubly degenerate), are 0.060, 0.052, 0.044 and 0.056 for the four **K** points, respectively.

4. Thermal equilibration at variable *p,T*

At a given temperature and pressure, the equilibrium unit cell and atomic coordinates are obtained by minimization of the Gibb's free energy. This is equivalent to searching for the crystal structure with zero forces acting on individual atoms, which undergoes lattice strains consistent with the external isotropic pressure. The program *PARAPOCS* carries out such a task by an iterative numerical procedure described in detail elsewhere (Pavese *et al.*, 1996). In summary, for a given pressure the unit-cell strains ε_1 and ε_3 are searched, which give derivatives $\partial F/\partial\varepsilon_i$ equal to lattice stresses

imposed by the external pressure. A converging iterative procedure, based on a linear approximation relating the first derivatives (stresses) to lattice strains (Newton method), is applied. At every step, the function is minimized *versus* atomic coordinates before calculating its second derivatives (elastic constants), which are the coefficients of the linear approximation. It should be emphasized that the computed stresses and elastic constants include the quasi-harmonic vibrational contribution (thermal pressure), derived by calculating the Grüneisen's parameters for all lattice-dynamical normal modes. In the present case, 216 points in the first Brillouin zone were considered, giving a total of 6480 vibrational modes included in the calculation.

The process of thermal equilibration was performed on α-Al_2O_3 at temperatures ranging from 300 to 1700 K with steps of 100 (at $p = 0$) or 200 K (at $p = 10, 20, 30, 40$ GPa). Further, in the case $T = 300$ K the additional pressure values $p = 2, 4, 6, 8, 15, 25, 35$ GPa were considered. Thus, an extensive grid of 54 values in the p,T space was explored, recording for each point the following physical quantities: lattice constants a, c, V, atomic coordinates x(O) and z(Al), elastic bulk moduli K_T and K_S, coefficient of thermal expansion α, Grüneisen's parameter γ and heat capacity C_p.† Further, the thermal properties at $p = 0$ and the baric ones at $T = 300$ K, which can be compared with available experimental results, were studied in greater detail by also considering the behaviour of individual elastic constants. Results obtained at room conditions are summarized in Table 3; atomic coordinates differ slightly from those of Table 2, where no thermal equilibration was applied. The x(O) coordinate refers to the oxygen core position; the shell x value is 0.32010 and corresponds to a core-shell separation of 0.015 Å.

Table 3. *Calculated and experimental structural, elastic (K_T, K_S) and thermal expansion (α) properties of α-Al_2O_3 at room conditions*

γ is Grüneisen's parameter. Experimental data: structure from Kirfel & Eichhorn (1990); other data from Goto & Anderson (1989).

	Calculated	Experimental
a (Å)	4.7577	4.757
c (Å)	12.9829	12.988
V (Å^3)	254.50	254.5
x(O)	0.32327	0.30627
z(Al)	0.34503	0.35220
K_T (GPa)	245.6	252.3
K_S (GPa)	247.2	253.7
α (10^{-6} K^{-1})	15.67	15.45
γ	1.269	1.277

5. Least-squares fits of the equation of state

It is very important that the dependence of simulated properties on p,T can be expressed by analytical approximation formulae, both for ease of use and for ease of deriving mathematically related physical quantities. In this context we chose least-squares polynomial approximations of the relative changes $r_{pT} = \Delta y_{pT}/y_{00} = (y_{pT} - y_{00})/y_{00}$; the values of $y_{00} = y(p = 0, T = 300$ K) are those reported in Table 3. The process $y_{00} \rightarrow y_{pT}$ can be split into two partial processes according to $y_{00} \rightarrow y_{p0}(T = 300$ K$) \rightarrow y_{pT}$, and the corresponding relative changes $r_p = \Delta y_{p0}/y_{00}$ and $r_T = \Delta y_{pT}/y_{p0}$ are defined. It turns out, by algebraic manipulation, that $r_{pT} = r_p + r_T + r_p r_T$. The r_p quantities were fitted to p-dependent polynomials and the r_T quantities to T-dependent polynomials with p-dependent coefficients.

For the lattice constants a, c and V, the $r_p r_T$ quantity turned out to be negligible with respect to $r_p + r_T$. Thus, the corresponding equation of state could be represented by

$$\begin{aligned}\Delta y_{pT}/y_{00} = {} & c_{10}p + c_{20}p^2 \\ & + (c_{01} + c_{11}p + c_{21}p^2)(T - 300) \\ & + (c_{02} + c_{12}p + c_{22}p^2)(T - 300)^2 \\ & + (c_{03} + c_{13}p + c_{23}p^2)(T - 300)^3. \quad (5)\end{aligned}$$

Similarly, for the atomic coordinates x(O) and z(Al) the following simpler approximation was derived:

$$\begin{aligned}\Delta y_{pT}/y_{00} = {} & c_{10}p + c_{20}p^2 \\ & + (c_{01} + c_{11}p + c_{21}p^2)(T - 300). \quad (6)\end{aligned}$$

The fitted values of all coefficients are reported in Table 4. The s.u.'s of coefficients are of the order of magnitude of the last decimal digit reported. For the sake of comparison with available experimental data, the results of pure thermal expansion at room pressure (Wachtman *et al.*, 1962) and of pure compression at room temperature (Richet *et al.*, 1988) were approximated by consistent least-squares polynomials $c_{01}(T - 300) + c_{02}(T - 300)^2 + c_{03}(T - 300)^3$ and $c_{10}p + c_{20}p^2$, respectively, for the former and the latter case. The corresponding coefficients are also reported in Table 4. Of course, in this case it is not possible to sum the pure p-dependent and T-dependent contributions to obtain the p,T effect on $\Delta y_{pT}/y_{00}$, as no mixed p,T experimental data are available to constrain the pressure dependence of thermal expansion.

In principle, from the fitted analytical $V(p,T)$ behaviour the temperature–pressure dependence of the thermal expansion coefficient $\alpha = (1/V)(\partial V/\partial T)_p$ and isothermal bulk modulus $K_T = -V(\partial p/\partial V)_T$ could also be obtained straightforwardly. However, the fitting numerical error propagates so unfavourably in the differentiation process that the ensuing values are affected by a large uncertainty, unless polynomials of

† Supplementary data for this paper are available from the IUCr electronic archives (Reference: SH0114). Services for accessing these data are described at the back of the journal.

Table 4. *Coefficients of the least-squares approximations [(5) and (6)] for the simulated p,T dependence of lattice constants and atomic coordinates of α-Al_2O_3*

Coefficients derived from experimental compression data at T = 300 K and thermal expansion data at zero pressure are also reported.

		a	c	V	x(O)	z(Al)
c_{10}		-1.357×10^{-3}	-1.137×10^{-3}	-3.819×10^{-3}	4.014×10^{-4}	-5.508×10^{-5}
	Experimental[(a)]	-1.26×10^{-3}	-1.18×10^{-3}	-3.65×10^{-3}		
c_{20}		8.46×10^{-6}	7.61×10^{-6}	2.65×10^{-5}	-2.43×10^{-6}	0
	Experimental[(a)]	8.8×10^{-6}	4.7×10^{-6}	2.4×10^{-5}		
c_{01}		6.04×10^{-6}	5.41×10^{-6}	1.76×10^{-5}	-2.36×10^{-6}	1.27×10^{-7}
	Experimental[(b)]	5.92×10^{-6}	6.71×10^{-6}	1.85×10^{-5}		
c_{11}		-1.12×10^{-7}	-1.11×10^{-7}	-3.43×10^{-7}	2.92×10^{-8}	5.25×10^{-9}
c_{21}		1.09×10^{-9}	1.08×10^{-9}	3.42×10^{-9}		
c_{02}		3.01×10^{-9}	2.84×10^{-9}	8.78×10^{-9}		
	Experimental[(b)]	3.13×10^{-9}	3.26×10^{-9}	9.73×10^{-9}		
c_{12}		5.6×10^{-11}	-5.8×10^{-11}	-1.5×10^{-10}		
c_{22}		6.8×10^{-13}	7.1×10^{-13}	1.7×10^{-12}		
c_{03}		-8.1×10^{-13}	-7.4×10^{-13}	-2.2×10^{-12}		
	Experimental[(b)]	-1.1×10^{-12}	-1.1×10^{-12}	-3.2×10^{-12}		
c_{13}		1.2×10^{-14}	1.3×10^{-14}	2.2×10^{-14}		
c_{23}		-1.3×10^{-16}	-1.6×10^{-16}	-1.8×10^{-16}		

References: (*a*) Richet *et al.* (1988); (*b*) Wachtman *et al.* (1962).

high order (with many parameters) are used to fit a, c and V data against p,T. We have chosen to limit the order of such polynomials [*cf.* (5)] to the minimum necessary to achieve a reasonable precision of lattice constants, at the expense of the precision of derivative quantities such as α and K_T. For these, the values directly output from the *PARAPOCS* (Pavese *et al.*, 1996) code were considered and used for the following independent polynomial fittings, whose coefficients are reported in Table 5. For both K_T and α

$$r_p = \Delta y_{p0}/y_{00} = c_{10}p + c_{20}p^2; \quad (7)$$

for K_T

$$r_T = \Delta y_{pT}/y_{p0} = (c_{01} + c_{11}p + c_{21}p^2)(T - 300); \quad (8)$$

for α

$$r_T = \Delta y_{pT}/y_{p0} = (c_{01} + c_{11}p)(T - 300) + (c_{02} + c_{12}p)(T - 300)^2 + (c_{03} + c_{13}p)(T - 300)^3. \quad (9)$$

In these cases the approximation $r_{pT} \simeq r_p + r_T$ proves not to be satisfactory and the general expression

$$\Delta y_{pT}/y_{00} = r_{pT} = r_p + r_T + r_p r_T \quad (10)$$

has to be employed for calculating changes of K_T and α owing to variations of p and T together, in order to achieve a reasonable numerical precision.

The precision of the polynomial fittings was evaluated by computing the deviations between fitted and original (from the output of *PARAPOCS*) values of $r_{pT} = \Delta y_{pT}/y_{00}$, where $y = a$, c, V, x(O), z(Al), K_T and α, for the whole data set of 54 points explored in the (p,T) space. The average per cent deviations (in absolute value) turn out to be 0.016, 0.015, 0.068, 0.009, 0.005, 0.206 and 1.462%, respectively, for each of the y quantities. Multiplication by the corresponding y_{00} values (Table 3) yields the absolute average errors owing to numerical fitting, which are surely smaller than the estimated errors of equivalent experimental determinations.

6. Discussion

In Table 3 the computed equilibrium values of lattice, structural, elastic and thermal expansion properties are compared with experimental results (Kirfel & Eichhorn, 1990; Goto & Anderson, 1989). The quality of the agreement observed at 300 K and zero pressure of course reflects the quality of the potential used; this performs excellently with the exception perhaps of the atomic coordinates, which show a slightly larger deviation. On the other hand, the behaviour of simulated properties at other temperatures and pressures is really predicted, because no experimental information at $T \neq 300$ K and $p \neq 0$ was included in the fitting of the potential. Results can be compared with the available measured quantities only for the temperature dependence at room pressure (lattice constants, bulk modulus and thermal expansion coefficient) and for the pressure dependence at room temperature (lattice constants and bulk modulus).

In Figs. 1 and 2 the relative changes $\Delta y_{pT}/y_{p0}$ of computed unit-cell edges and volume are plotted *versus* temperature for each of the five pressure values considered; the corresponding experimental data at room pressure of Wachtman *et al.* (1962) and Touloukian *et al.* (1977) are also shown. With respect to the first set of measurements, calculated results show a slight under- and overestimate, respectively, for the thermal

expansion of the a and c cell edges, while the volume is reproduced in an excellent way. This is confirmed by consideration of the coefficients c_{01}, c_{02} and c_{03} of the numerical fittings of (5) for $p = 0$, as they are reported in Table 4 for both theoretical and experimental data. The measured results of the second set give a perfect agreement for the a cell edge, while both c and V show slightly larger thermal expansions than the corresponding computed values. Absolute deviations of theoretical *versus* experimental a and c edges increase constantly with T and attain maximum values (at 1700 K) of 0.004 and -0.025 Å, respectively, with respect to the data of Wachtman *et al.* (1962) and of -0.002 and -0.038 Å with respect to the results of Touloukian *et al.* (1977). As for V, the maximum deviations are -0.2 Å^3 at 1200 K and -1.0 Å^3 at 1700 K for the two sets of experimental data, respectively. These results, showing errors of the order of 0.1% over the whole temperature range, can be considered to be very good and to approach the order of accuracy obtained in routine measurements.

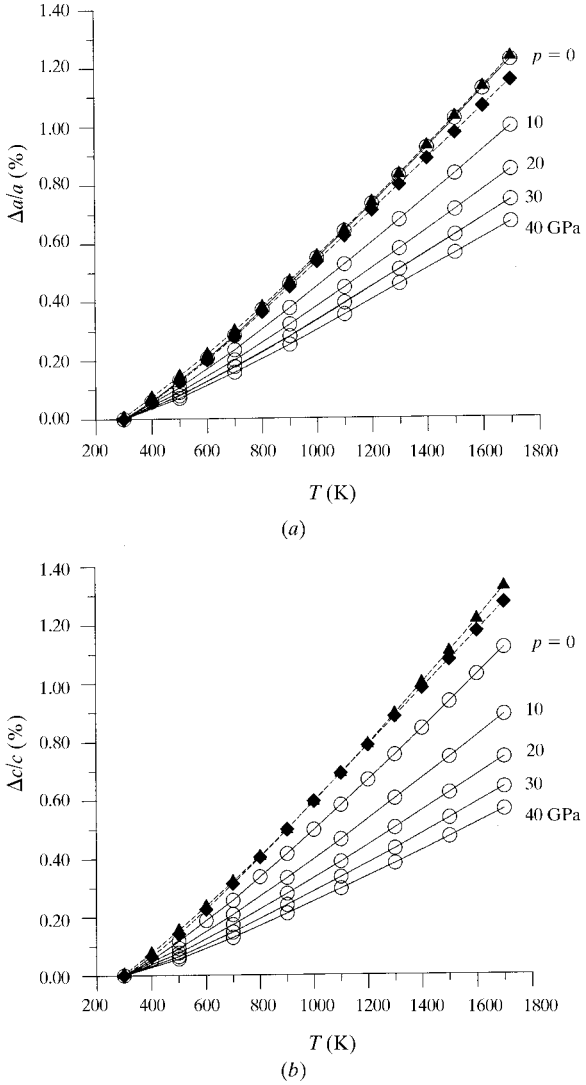

Fig. 1. Thermal dependence of the calculated (○) (*a*) a and (*b*) c lattice constants of α-Al_2O_3 at several pressures. Experimental values at room pressure (◆ Wachtman *et al.*, 1962; ▲ Touloukian *et al.*, 1977) are also shown.

Graphs of the relative changes $\Delta y_{pT}/y_{0T}$ of computed a, c and V against pressure are shown in Figs. 3 and 4, for $T = 300$, 1100 and 1700 K. Therein, they are compared with experimental results at room temperature by Sato & Akimoto (1979), SA, and by Richet *et al.* (1988), R, in the ranges 0–12 and 0–41 GPa, respectively. One can notice that SA results, extrapolated to higher pressure, would indicate a larger compressibility than that shown by both R data and our own calculated results. Indeed the computed volume V shows an excellent agreement with R experimental values, with deviations well within the error bars. Slightly larger, but hardly significant, deviations are observed for the individual a and c cell edges, with a small over- and underestimate of the corresponding compressibilities, respectively, just as was the case for thermal expansion results. This analysis is supported by examination of the parabolic fit coefficients c_{10} and c_{20} of theoretical and experimental (R) lattice constants *versus* pressure at $T = 300$ K (Table 4).

As for the theoretical bulk modulus K_T and thermal expansion coefficient α, we have chosen to plot their absolute values, rather than relative changes, against T for every pressure value (Figs. 5 and 6, respectively). Measured data at $p = 0$ are shown for comparison. The predicted slope of $K_T(T)$ at room pressure is almost constant and agrees excellently with the experimental one. On the other hand, the slope of the calculated $\alpha(T)$ function at $p = 0$ decreases, with increasing T, less rapidly than that of the measured curve. However, the

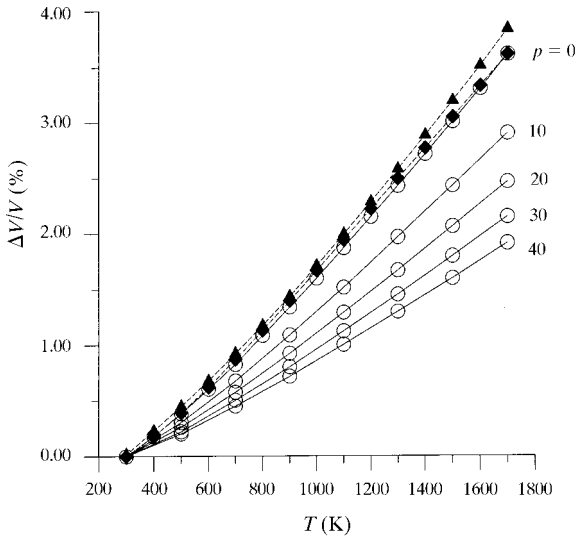

Fig. 2. As in Fig. 1, but for the unit-cell volume V.

ensuing changes of α are small enough to give an average relative error of 6% over the whole T range considered, with the maximum value below 10%. This is a remarkable achievement of this work, taking into account that the thermal expansion coefficient is a very delicate quantity to predict accurately on the basis of atomistic calculations.

The most interesting results of the present investigation concern the predicted coupled p,T dependence of lattice constants, bulk modulus and thermal expansion coefficient of α-Al_2O_3, as no corresponding experimental data are available. This behaviour can be assessed qualitatively by looking at Figs. 5 and 6. To a first approximation the bulk modulus K_T shows a linear dependence on temperature with a slope almost independent of pressure (Fig. 5). Indeed, the $K_T(p,T)$ polynomial fit given by (7), (8) and (10) is, to first order of the $p(T-300)$ term,

$$K_T \simeq K_{00}[1 + c_{10}p + c_{20}p^2 + c_{01}(T-300) + (c_{11} + c_{10}c_{01})p(T-300)]. \quad (11)$$

The coefficient of the p,T coupling term is $(1/K_{00})\partial^2 K_T/\partial p\partial T = c_{11} + c_{10}c_{01}$; this has a value of 3.4×10^{-7} GPa^{-1} K^{-1} (Table 5) and appears to be quite small, consistent with the behaviour shown by Fig. 5. On the other hand, the thermal expansion coefficient has a strongly non-linear coupled dependence on T and p, as shown by Fig. 6. A knowledge of the slopes of the $\alpha(p)$ and $K_T(T)$ curves is also very useful to characterize the

Table 5. *Coefficients of the least-squares approximations [(7)–(10)] for the simulated p,T dependence of the isothermal bulk modulus K_T and coefficient of thermal expansion α of α-Al_2O_3*

		K_T	α
c_{10}		1.932×10^{-2}	-2.008×10^{-2}
	Experimental[a]	1.976×10^{-2}	
c_{20}		-3.30×10^{-5}	2.14×10^{-4}
c_{01}		-1.245×10^{-4}	2.009×10^{-3}
	Experimental[b]	-1.17×10^{-4}	2.53×10^{-3}
c_{11}		2.75×10^{-6}	1.45×10^{-5}
c_{21}		-3.0×10^{-8}	0
c_{02}		0	-1.96×10^{-6}
	Experimental[b]		-2.73×10^{-6}
c_{12}		0	-1.58×10^{-8}
c_{03}		0	7.1×10^{-10}
	Experimental[b]		9.6×10^{-10}
c_{13}		0	4.6×10^{-12}

References: (*a*) Richet *et al.* (1988); (*b*) Goto & Anderson (1989).

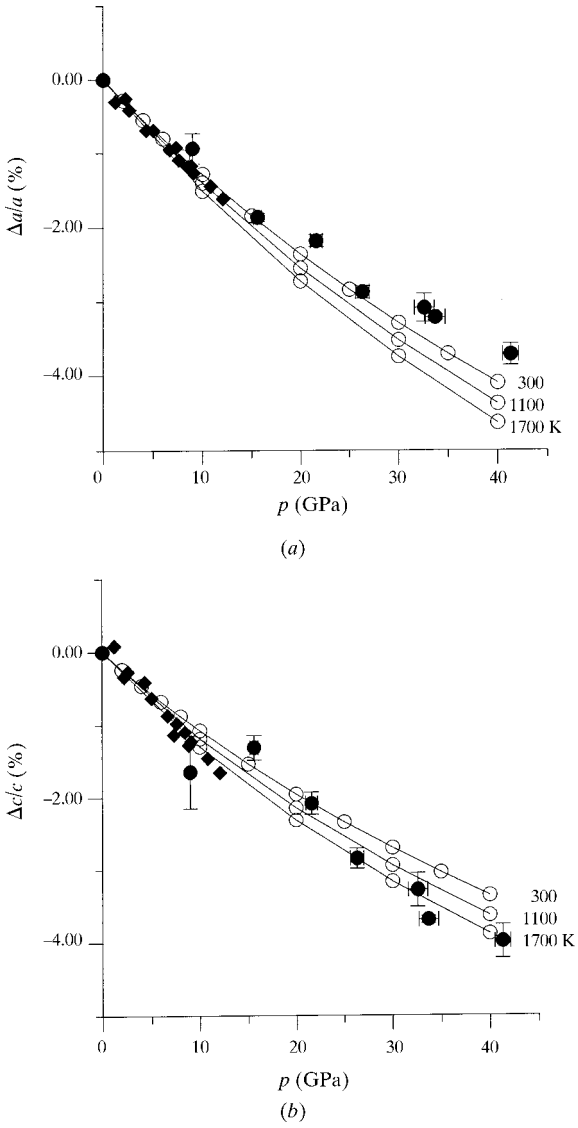

Fig. 3. Pressure dependence of the calculated (○) (*a*) *a* and (*b*) *c* lattice constants of α-Al_2O_3 at three different temperatures. Experimental values at room temperature (◆ Sato & Akimoto, 1979; ● Richet *et al.*, 1988) are also shown.

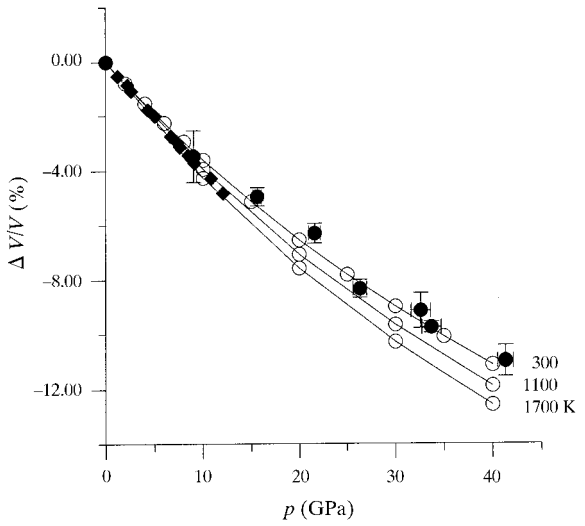

Fig. 4. As in Fig. 3, but for the unit-cell volume *V*.

Table 6. *For each pair of p,T values, the computed quantities* $(\partial\alpha/\partial p)_T$ *and* $(1/K_T^2)(\partial K_T/\partial T)_p$ *(first line), and their average representing* $(1/V)\partial^2 V/\partial p\partial T$ *(second line) are reported* ($10^{-7}GPa^{-1}K^{-1}$)

	T = 300	T = 900 K	T = 1300 K	T = 1700 K
p = 0 GPa	−3.5; −4.4	−5.0; −6.1	−5.8; −7.2	−6.9; −8.2
	−3.9	−5.6	−6.5	−7.5
p = 10 GPa	−2.4; −2.8	−3.5; −3.9	−3.9;−4.3	−4.4; −4.4
	−2.6	−3.7	−4.1	−4.4
p = 20 GPa	−1.6; −2.1	−2.4; −2.8	−2.6; −3.1	−2.8; −3.3
	−1.9	−2.6	−2.8	−3.0
p = 30 GPa	−1.2; −1.5	−1.7; −2.1	−1.9; −2.3	−2.0; −2.3
	−1.4	−1.9	−2.1	−2.2
p = 40 GPa	−1.1; −1.2	−1.6; −1.7	−1.7; −1.8	−2.0; −1.8
	−1.2	−1.6	−1.8	−1.9

pressure–temperature coupling behaviour of the unit-cell volume, by means of the thermodynamic equations

$$(1/V)\partial^2 V/\partial p\partial T = (\partial\alpha/\partial p)_T = (1/K_T^2)(\partial K_T/\partial T)_p. \quad (12)$$

As stressed above in the section on least-squares fittings, derivatives obtained by analytical differentiation of the given polynomial approximations [(5)–(10), Table 5] give a poor numerical precision, because the order of polynomials is not high enough for that purpose. Thus, the two first derivatives in (12) were calculated by performing higher order (cubic) fits of $\alpha(p)$ (at different temperatures) and of $K_T(T)$ (at different pressures), respectively. The results are given numerically for five p and four T values in Table 6. One can notice that the equality of the two derivatives is not strictly obeyed, but there are slight differences which tend to vanish at high pressure. Owing to the very careful procedure followed for numerical differentiation, we believe that these differences are related to the intrinsic approximations and numerical errors of the *PARAPOCS* calculations, rather than to the polynomial fittings. Indeed (12) is a severe test for the computational method used, taking into account the different ways α and K_T are computed and the complexity of the thermal equilibration procedure. The results obtained are satisfactory, considering that the average relative deviation from the mean of the two derivatives amounts to 7.6%. The mean values reported in Table 6 can be considered as the best approximation to $(1/V)\partial^2 V/\partial p\partial T$ and allow one to predict the full coupled p,T behaviour of the α-Al_2O_3 equation of state. In particular, it turns out that at low p and high T the pressure coefficient of α is far from negligible, so that the thermal expansion of alumina is reduced significantly by increasing p. This effect is much smaller, on the other hand, in conditions of low temperature and high pressure.

7. Conclusions

The quasi-harmonic approach for simulating structural and thermodynamic properties of solids at high

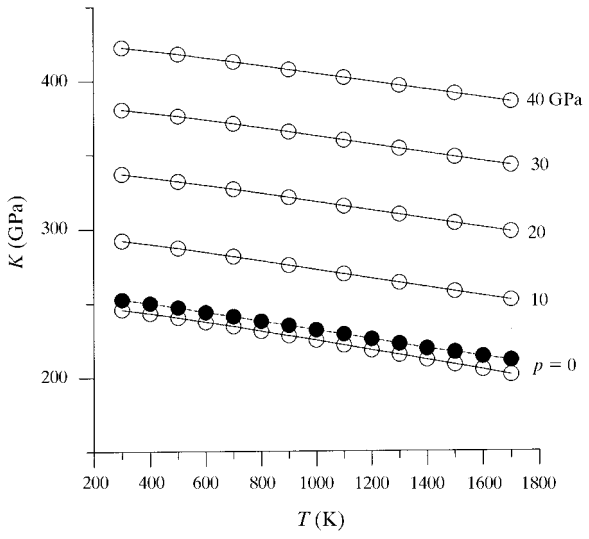

Fig. 5. Thermal dependence of the calculated (○) and experimental (● Goto & Anderson, 1989) isothermal bulk modulus of α-Al_2O_3 at different pressures.

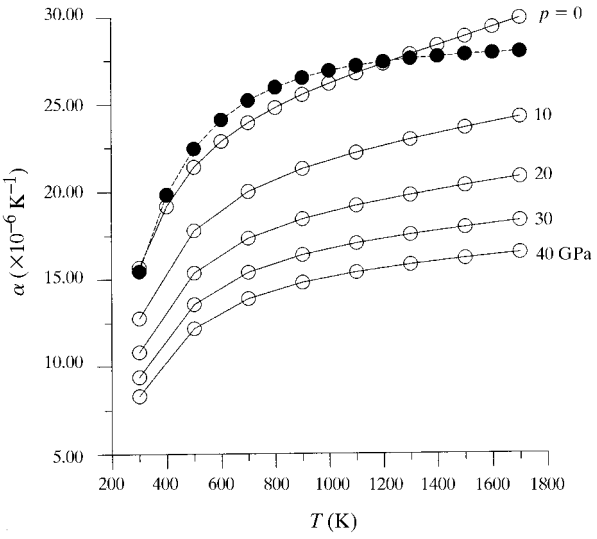

Fig. 6. Thermal dependence of the calculated (○) and experimental (● Goto & Anderson, 1989) coefficient of thermal expansion of α-Al_2O_3 at different pressures.

temperature and pressure has been applied successfully to α-Al_2O_3. By using an interatomic potential fitted to room-p,T measured data, it was possible to predict correctly the equation of state at room temperature/high pressure and at room pressure/high temperature, in very good agreement with experiment. Furthermore, the coupled p,T dependence of all lattice and elastic properties was also calculated, so as to provide a set of relevant theoretical results which compensate for missing experimental data. In particular, knowing the pressure dependence of thermal expansion is very important for several applications of refractory materials and quasi-harmonic simulations have proved to provide an attractive alternative to difficult measurements.

This work was supported financially by the Ministero Università e Ricerca Scientifica e Tecnologica, Roma.

References

d'Amour, H., Schiferl, D., Denner, W., Schulz, H. & Holzapfel, W. B. (1978). *J. Appl. Phys.* **49**, 4411–4416.

Born, M. & Huang, K. (1954). *Dynamical Theory of Crystal Lattices*. Oxford: Clarendon Press.

Brown, N. E., Swapp, S. M., Bennet, C. L. & Navrotsky, A. (1993). *J. Appl. Cryst.* **26**, 77–81.

Catlow, C. R. A., James, R., Mackrodt, W. C. & Stewart, R. F. (1982). *Phys. Rev. B*, **25**, 1006–1026.

Catti, M., Pavese, A. & Price, G. D. (1993). *Phys. Chem. Miner.* **19**, 472–479.

Goto, T. & Anderson, O. L. (1989). *J. Geophys. Res.* **94**, 7588–7602.

Hull, S., Keen, D. A., Done, R., Pike, T. & Gardner, N. J. G. (1997). *Nucl. Instr. Methods Phys. Res. A*, **385**, 354–360.

Ishizawa, N., Miyata, T., Minato, I., Marumo, F. & Iwai, S. (1980). *Acta Cryst.* B**36**, 228–230.

James, F. & Roos, M. (1975). *Comput. Phys. Commun.* **10**, 343–367.

Jephcoat, A. P., Hemley, R. J. & Mao, H. (1988). *Physica B*, **150**, 115–121.

Kappus, W. (1975). *Z. Phys. B*, **21**, 325–331.

Kirfel, A. & Eichhorn, K. (1990). *Acta Cryst.* A**46**, 271–284.

Lewis, J., Schwarzenbach, D. & Flack, H. D. (1982). *Acta Cryst.* A**38**, 733–739.

Parker, S. C. & Price, G. D. (1989). *Adv. Solid State Chem.* **1**, 295–327.

Pavese, A., Catti, M., Parker, S. C. & Wall, A. (1996). *Phys. Chem. Miner.* **23**, 89–93.

Richet, P., Xu, J. & Mao, H. (1988). *Phys. Chem. Miner.* **16**, 207–211.

Sato, Y. & Akimoto, S. (1979). *J. Appl. Phys.* **50**, 5285–5291.

Schober, H., Strauch, A. & Dorner, B. (1993). *Z. Phys. B*, **92**, 273–283.

Touloukian, Y. S., Kirby, R. K., Taylor, R. E. & Lee, T. Y. R. (1977). *Thermophysical Properties of Matter*, Vol. 13. New York: Plenum Press.

Wachtman, J. B. Jr, Scuderi, T. G. & Cleek, G. W. (1962). *J. Am. Ceram. Soc.* **45**, 319–323.

Yates, B., Cooper, R. F. & Pojur, A. F. (1972). *J. Phys. C*, **5**, 1046–1058.

Zhang, J., Martinez, I., Guyot, F., Gillet, P. & Saxena, S. K. (1997). *Phys. Chem. Miner.* **24**, 122–130.